Nuclear Engineering and Technology 54 (2022) 429–436

Contents lists available at ScienceDirect

Nuclear Engineering and Technology

journal homepage: www.elsevier.com/locate/net

Original article

Thermally assisted IRSL and VSL measurements of display glass from mobile phones for retrospective dosimetry

Michael Discher [a, *], Hyoungtaek Kim [b], Jungil Lee [b]

[a] Paris-Lodron-University of Salzburg, Department of Geography and Geology, Salzburg, Austria
[b] Korea Atomic Energy Research Institute, Radiation Safety Management Division, Yuseong, Daejeon, Republic of Korea

ARTICLE INFO

Article history:
Received 15 April 2021
Received in revised form
18 June 2021
Accepted 16 July 2021
Available online 18 July 2021

Keywords:
Thermally assisted OSL
Retrospective dosimetry
Dosimetric properties
Display glass of mobile phones

ABSTRACT

Investigations of retrospective dosimetry have shown that components of mobile phones are suitable as emergency dosimeters in case of radiological incidents. For physical dosimetry, components can be read out using optically stimulated luminescence (OSL), thermoluminescence (TL) and phototransferred thermoluminescence (PTTL) methods to determine the absorbed dose. This paper deals with a feasibility study of display glass from modern mobile phones that are measured by thermally assisted (Ta) optically stimulated luminescence. Violet (VSL, 405 nm) and infrared (IRSL, 850 nm) LEDs were used for optical stimulation and two protocols (Ta-VSL and Ta-IRSL) were tested. The aim was to systematically investigate the luminescence properties, compare the results to blue stimulated Ta-BSL protocol (458 nm) and to develop a robust measurement protocol for the usage as an emergency dosimeter after an incident with ionizing radiation.

First, the native signals were measured to calculate the zero dose signal. Next, the reproducibility and dose response of the luminescence signals were analyzed. Finally, the signal stability was tested after the storage of irradiated samples at room temperature. In general, the developed Ta-IRSL and Ta-VSL protocols indicate usability, however, further research is needed to test the potential of a new protocol for physical retrospective dosimetry.

1. Introduction

The possibility of accidental exposure of civilians and radiation workers is generally increased by the use of ionizing radiation sources in the field of medicine, industry and research. Beyond that, attention is given to intentional exposure due to a radiological attack with a possible high number of exposed people. In such an event, the dosimetric triage using methods of physical and biological retrospective dosimetry is extremely important to identify the people with high exposures and to distinguish them from the lower and non-exposed. Most of the methods of retrospective dosimetry are based on the measurement of the radiation damage induced in tissues, mainly blood cells but also teeth and nails [1,2] or in personal items worn by the individual [3–5]. The possibility to use personal objects as individual dosimeters has been successfully investigated, i.e. such as chip cards and electronic devices, in particular, electronic components mounted on a circuit board, like resistors, inductors or resonators [6–17]. Various studies were carried out on glass extracted from display screens of mobile phones using thermoluminescence (TL) and phototransferred thermoluminescence (PTTL) methods to determine the absorbed dose. The dosimetric properties were investigated for display glasses [18–25], touchscreen glasses [26–28] and protective glasses of modern mobile phones [29,30]. A good signal reproducibility and a linear dose response were observed. Additionally, the photon energy dependence and angular response were experimentally investigated for different display glasses used in mobile phones [19,20] and experimental results were validated using radiation transport simulations [31]. The studies showed that a native signal, so-called zero dose signal, is observed for unexposed glass samples which significantly limits the low-dose sensitivity. This zero dose signal could be reduced by employing a labor-intensive sample preparation procedure [23]. In contrast to the PTTL signal of glasses, the TL signal of glasses is not stable over time and a fading correction has to be applied for an accurate dose reconstruction.

In this study, we further investigated the approach using the novel thermally assisted OSL (Ta-OSL) protocol for dose assessment of display glasses, which was introduced by Kim et al. [32], in order

* Corresponding author.
E-mail address: Michael.Discher@sbg.ac.at (M. Discher).

https://doi.org/10.1016/j.net.2021.07.027

to achieve a reduced fading rate as well as lower intrinsic zero dose signal. One of the important protocol parameters of the previously mentioned Ta-OSL study is the choice of the stimulation wavelength. This paper deals with the dosimetric properties of display glass using thermally assisted OSL protocols using violet (Ta-VSL) and infra-red (Ta-IRSL) LEDs instead of blue (Ta-BSL) LEDs as stimulation wavelengths. The aim of the study is to extend the research and to provide a systematic investigation of dosimetric properties in order to develop a robust measurement protocol.

2. Materials and methods

In this study representative glass samples of a modern mobile phone (Samsung Galaxy S3) with an AMOLED (active-matrix organic light-emitting diode) display technology were used. The glass aliquots indicate the typical broad TL glow curve of lime-aluminosilicate glasses and belong to glass category A, according to the display glass classification given in Discher and Woda [24]. Following the sample preparation given in Discher et al. [23] the glass aliquots were etched for 4 min by concentrated hydrofluoric acid (HF; 48%) to remove the thin AMOLED layer, subsequently the pure substrate glass was cleaned with ethanol and cut into pieces of approx. 5×5 mm^2, suitable for fitting into the stainless steel cups of the luminescence reader.

An automated reader Lexsyg Research made by Freiberg Instruments [33] was used to carry out the luminescence measurements. A built-in Sr-90/Y-90 beta source (norm. activity of 1.51 MBq) was used, delivering an absorbed dose rate in SiO_2 of $\approx$0.058 Gy/s for laboratory irradiations and calibrated against a secondary standard Cs-137 gamma source. The reader is equipped with an optical stimulation module containing three stimulation wavelengths: violet LEDs (405 $\pm$ 3 nm), blue LEDs (458 $\pm$ 5 nm) and IR LEDs (850 $\pm$ 20 nm). Optical powers of 80 mW/cm^2 (violet), 100 mW/cm^2 (blue) and 200 mW/cm^2 (IR) at the sample position are available for optical stimulation. The luminescence signals are detected with a bialkali cathode photomultiplier tube Hamamatsu H7360-02. To block scattered stimulation light during optical stimulation and thermal background signals during heating, a combination of glass filters (Schott BG39, Schott BG 25, Schott KG3) is available for the IRSL measurements to get a broad detection window (wideband blue) with a center wavelength of 400 nm including a full width at half maximum (FWHM) of approx. 100 nm. For the violet stimulation a combination of a glass and interference filter is used (Schott KG3, AHF-BrightLine HC340/26 interference) with a detection window of 340 nm (center wavelength) and a FWHM of approx. 30 nm.

All luminescence measurements at elevated temperatures were performed in a N_2 atmosphere. The heating rate was set to 5 °C/s to reach the readout temperature (i.e. 100, 200 or 300 °C) and a hold time of 10 s was always included for temperature stabilization. The duration of the optical stimulation was fixed to 500 s. After each optically stimulated luminescence readout the sample was quickly annealed to 450 °C with a heating rate of 10 °C/s and hold for 10 s to delete residual luminescence signals. Only one glass aliquot was used for each protocol and test to investigate the dosimetric properties (i.e. dose response, signal stability and optical stability tests) due to the high reproducibility behavior. For the analysis, generally, the recorded signals were integrated between 0 and 50 s and an early background correction (50–100 s) were applied by simply subtracting both integration intervals.

3. Results and discussions

3.1. Zero dose signal

In this study the readout temperatures of the Ta-VSL and Ta-IRSL protocols were varied between 100 and 300 °C to investigate the effect on the intrinsic zero dose signal of unirradiated (unused) glass aliquots, which are needed because the zero dose signals are deleted after the first TL readout. It is assumed that the intrinsic signals are similar because the glass aliquots were extracted from the same mobile phone and were located adjacent to each other on the display [18]. First, the zero dose signal was recorded, then the aliquots were exposed to 1 Gy and the same readout protocol was applied again.

The zero dose and the radiation-induced signals (ca. 1 Gy) are shown in Fig. 1 a-f for the different stimulation wavelengths and readout temperatures.

The net signals of the decay curves indicate a strong signal

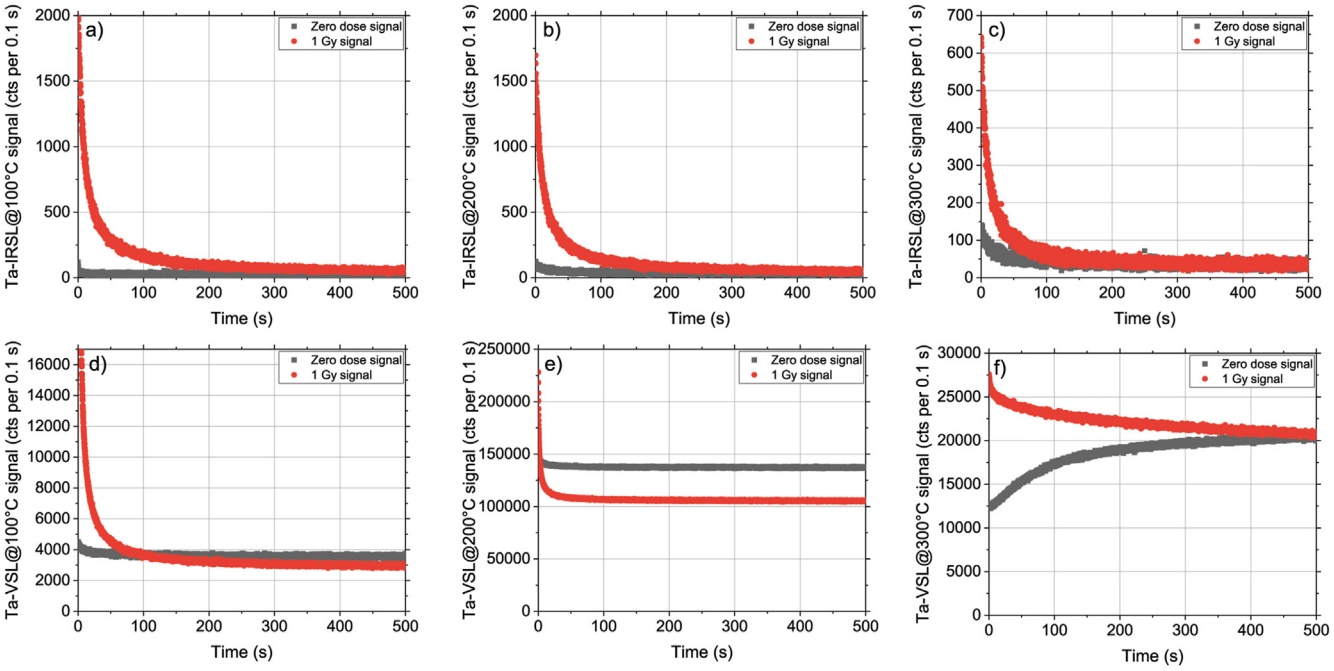

Fig. 1. a–f: Ta-IRSL and Ta-VSL measurements of the zero dose signal and the radiation induced signal after 1 Gy irradiation of a fresh glass sample.

Table 1
Calculated zero dose for the used protocol at different readout temperatures.

Protocol	Readout temperature		
	100 °C	200 °C	300 °C
Ta-IRSL	0.007 Gy	0.046 Gy	0.164 Gy
Ta-VSL	0.011 Gy	0.136 Gy	–

sensitivity for the Ta-VSL protocol. The intrinsic zero dose signal is transformed to a zero dose using the 1 Gy signal as a calibration dose and the corresponding integration intervals. The results are given in Table 1 for the Ta-IRSL and Ta-VSL measurements.

Generally, the zero doses are relatively low for both protocols and increase with increasing readout temperatures, which was also found for the Ta-BSL measurements in Kim et al. [32]. This result strengthens the hypothesis that the traps responsible for the native signals of display glasses have a lower thermo-optical cross-section than those of radiation induced signals.

For the Ta-VSL@300°C protocol, the zero dose is not calculated because of the unexpected build up shape of the decay curve and the lacking dosimetric properties, which are discussed further below. The phenomenon of the signal build up may be explained by a simultaneous thermal and optical transfer of trapped charges originated from the intrinsic zero dose signal and/or the accumulation of charges in deep traps occurs due to the violet stimulation, which are released in the course of time during the Ta-VSL measurement at high temperature. Further studies are necessary to investigate this phenomenon.

3.1.1. Detailed discussion of the decay curves

The decay curves acquired after the 1 Gy irradiation were normalized to the first channel and displayed in Fig. 2 a and b. The

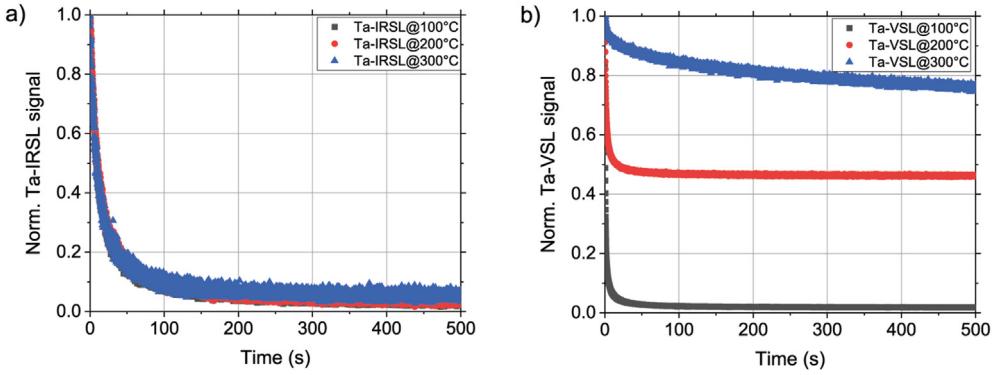

Fig. 2. a–b: Normalized decay curves of the Ta-IRSL (a) and Ta-VSL (b) measurements after 1 Gy irradiation using different readout temperatures.

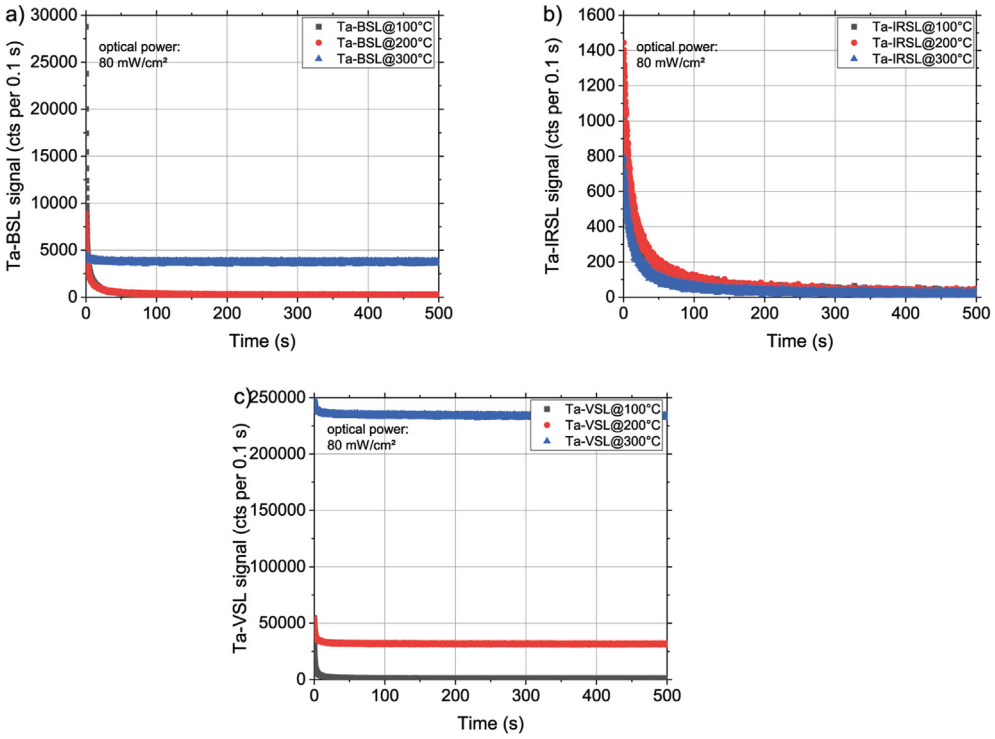

Fig. 3. a–c: Ta-OSL curves of the same sample for different stimulation modes and readout temperatures. The beta dose was always 1 Gy before the measurement and the optical power was fixed at 80 mW/cm^2 for a better comparison.

normalization was necessary because different glass aliquots were used. For the Ta-IRSL decay curves (Fig. 2 a) the shape is very similar and independent of the readout temperature. On the other hand, the Ta-VSL decay curves (Fig. 2 b) indicate a quick decay for 100 and 200 °C readout temperatures. A baseline shift is observed which is increased for higher readout temperatures. This baseline shift can be explained by a flat natural Ta-OSL (NTA-OSL) component, which is considered as the slow decaying component assisted by an activation process with an activation energy up to 1 eV [34,35] and which was also observed for the Ta-BSL with blue stimulation [32].

3.2. Comparison and deconvolution of the decay curves

For the direct comparison of the Ta-IRSL and Ta-VSL measurements it is useful to deconvolute the decay curves and to calculate the decay parameters. For this purpose, only one glass sample was selected, the given dose was always 1 Gy and the stimulation power of 80 mW/cm^2 was fixed, which is the maximum optical power for violet stimulation. Additionally, Ta-BSL measurements using the blue wavelength were recorded for further comparison.

The decay curves of the Ta-OSL protocols with different stimulation LEDs are displayed in Fig. 3. The Ta-BSL protocol indicates a systematic decrease of the signal intensity and a systematic increase of the offset with increasing readout temperatures. Such obvious trends are not observed for the Ta-IRSL protocol. Ta-VSL protocol implies a distinct increase of the offset with increasing readout temperatures.

In Fig. 4 the decay curves of the different protocols are displayed together which are normalized to the first channel. The shape of the decay curves can be deeply investigated and are deconvoluted by three simple exponential decay functions ($y = A_1*\exp(-x/t_1) + A_2*\exp(-x/t_2) + A_3*\exp(-x/t_3) + y0$). The parameters, standard errors and statistic results are summarized in Table 2. The offset relatively to the first channel was determined by the y_0 parameter.

The signal offsets are negligible for the Ta-IRSL protocols and the maximum shift is observed for the Ta-VSL@300°C protocol. Based on the measurements, NTA-OSL signals are increased with the temperature and energy of stimulation photons. The observed offsets could be explained by the already mentioned NTA-OSL component and by a simultaneous thermal and optical transfer of trapped charges, which is reinforced for higher readout temperatures.

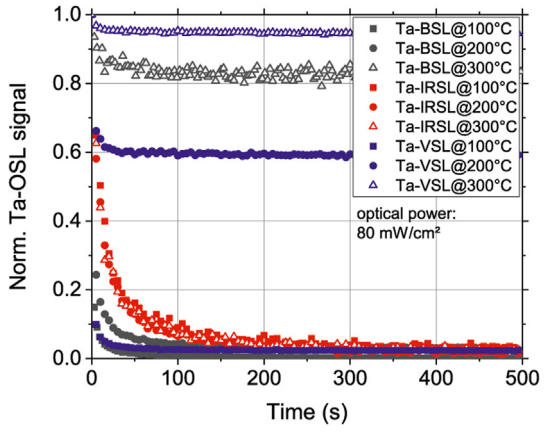

Fig. 4. Comparison of the normalized Ta-OSL decay curves.

Table 2
Calculated parameters of the deconvolution analysis of the normalized decay functions.

	y0		y0		A1		t1		A2		t2		A3		t3		Statistics	
	Value	Standard Error	Value	Standard Error	Value	Standard Error	Value	Standard Error	Value	Standard Error	Value	Standard Error	Value	Standard Error	Value	Standard Error	Reduced Chi-Sqr	Adj. R-Square
Ta-BSL@100°C	0.003	2.55E-05	0.258	0.001	3.51	0.02	0.845	0.002	0.44	0.00	0.049	3.26E-04	39.54	0.28	2.13E-06	0.99799		
Ta-BSL@200°C	0.031	5.36E-05	0.304	0.002	7.13	0.06	0.631	0.002	0.92	0.01	0.076	7.74E-04	53.58	0.51	7.29E-06	0.99700		
Ta-BSL@300°C	0.825	4.10E-04	0.096	0.008	12.30	1.48	0.091	0.010	1.74	0.35	0.018	3.43E-03	90.43	19.01	1.87E-04	0.57828		
Ta-IRSL@100°C	0.027	4.15E-04	0.483	0.014	5.54	0.15	0.404	0.012	20.81	0.71	0.140	4.49E-03	110.12	3.23	8.15E-05	0.99365		
Ta-IRSL@200°C	0.019	2.87E-04	0.449	0.009	5.16	0.11	0.400	0.007	20.67	0.50	0.118	3.43E-03	105.83	2.71	4.44E-05	0.99594		
Ta-IRSL@300°C	0.025	3.56E-04	0.420	0.012	4.69	0.15	0.452	0.010	19.61	0.59	0.125	5.14E-03	96.71	3.26	9.02E-05	0.99231		
Ta-VSL@100°C	0.024	2.13E-05	0.303	0.002	2.29	0.02	0.843	0.002	0.33	0.00	0.049	4.02E-04	24.20	0.20	1.77E-06	0.99784		
Ta-VSL@200°C	0.591	7.93E-05	0.280	0.003	0.83	0.02	0.124	0.002	6.57	0.16	0.018	5.90E-04	72.79	2.81	1.17E-05	0.96543		
Ta-VSL@300°C	0.945	9.39E-05	0.035	0.002	1.65	0.16	0.021	0.002	7.97	0.75	0.009	1.89E-04	140.81	6.67	3.78E-06	0.83951		

3.3. Reproducibility tests

Seven cycles of irradiation (1 Gy) and readouts were repeated using the different protocols to test the reproducibility for annealed glass aliquots. The integrated signals are normalized to the mean value of the seven cycles.

The reproducibility for the Ta-IRSL protocol, shown in Fig. 5 a, is in the range between 0.97 and 1.03 for the investigated readout temperatures (100, 200 and 300 °C). For the Ta-VSL protocol (Fig. 5 b) the reproducibility ranges between 0.93 and 1.06 for readout temperatures 100 and 200 °C, however, the Ta-VSL@300°C protocol indicates a systematical sensitivity change. There is a general tendency that the sensitivity decreases with increasing readout cycles (except for Ta-VSL@300°C protocol).

3.4. Dose response tests

The glass aliquots were exposed to beta doses between 0.12 and 7.4 Gy to obtain the dose response curves of the different protocols. In Fig. 6 a-b the decay curves after different beta irradiations for two selected protocols are shown.

A strong linear correlation ($R^2 > 0.99932$) is observed for the Ta-IRSL protocol for all three readout temperatures within the investigated dose range in Fig. 7 a. Similar results are received for the Ta-

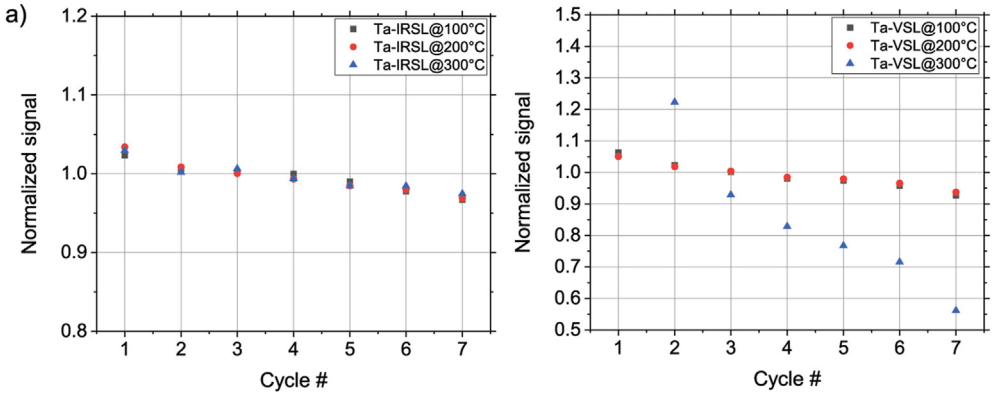

Fig. 5. a–b: Reproducibilty for the Ta-IRSL and Ta-VSL protocols at different readout temperatures using a 1 Gy test dose. The values are normlized to the mean of the seven repeated measurement and readout cycles.

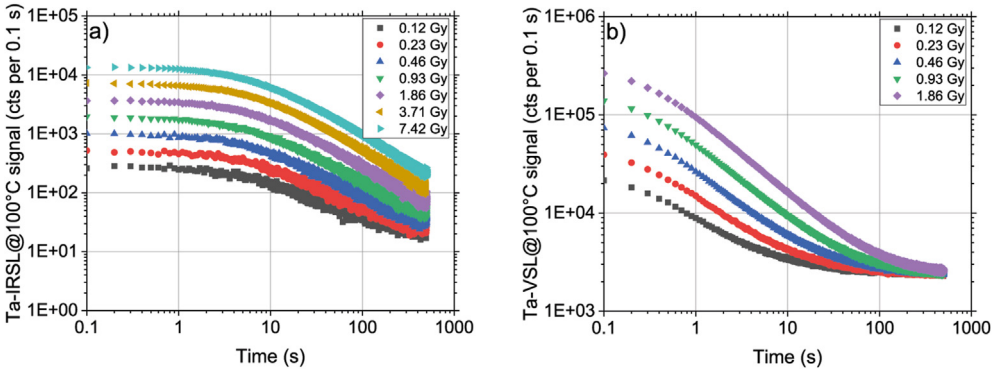

Fig. 6. a–b: Decay curves of the Ta-IRSL (a) and Ta-VSL (b) protocol after different beta irradiations.

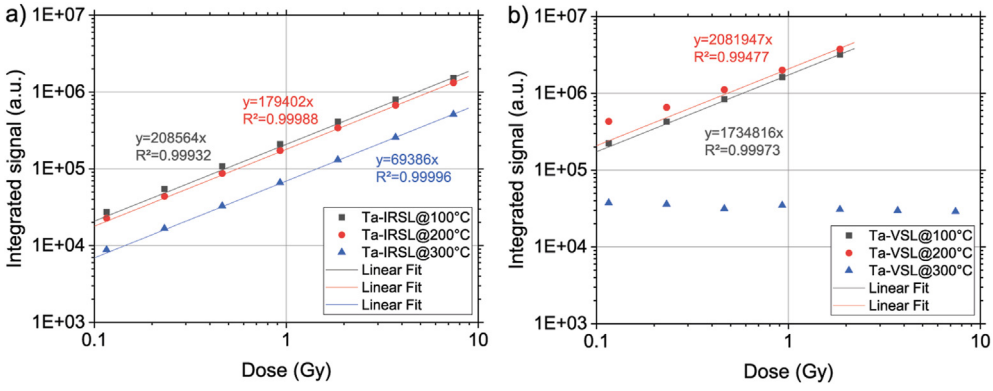

Fig. 7. a–b: Dose response of the Ta-IRSL (a) and Ta-VSL (b) protocol.

VSL@100°C and Ta-VSL@200°C protocol in Fig. 7 b. However, the Ta-VSL@300°C protocol does not indicate a signal increase with dose and fails to observe a linear response.

The maximum beta exposure for the Ta-VSL protocol at 100 and 200 °C was ca. 2 Gy due to the strong signal sensitivity of the protocol. Beta irradiations above 2 Gy caused overexposures of the PMT of the reader.

3.5. Signal stability test

One glass aliquot was used for testing the signal stability for each Ta-IRSL and Ta-VSL protocol according to the readout temperatures. After an irradiation (ca. 1 Gy) the aliquots were stored in the dark at ambient temperatures. After a storage time of about one week (7.2 days) the faded signals were recorded and after a second irradiation with the same dose the prompt signal was recorded. The faded signals were normalized to the second measurement carried out promptly after the irradiation step (time lag lies within a few seconds). The decay curves are displayed in Fig. 8. Using the usual integration interval the remained signals were calculated and the results of the signal stability tests are shown in Table 3.

The stability tests indicate that the signal stability is correlated to the readout temperatures. For the Ta-IRSL and Ta-VSL protocol the signal is more stable at higher readout temperatures. The highest signal loss is observed for the Ta-IRSL@100°C protocol (ca. 92% compared to the prompt readout). The Ta-VSL protocols prove a more stable signal and remained signals are calculated between 0.60 and 0.95. More investigations of different glass aliquots of various mobile phones are necessary to test the variability of the signal stability.

3.6. Optical stability test

For testing the optical stability one glass aliquot was used for each Ta-IRSL and Ta-VSL protocol with different readout temperatures. Additionally the pre-bleached TL protocol [24] was included for a comparison. After an irradiation (ca. 1 Gy) the aliquots were bleached for 500 s with the blue LEDs of the reader with the maximum optical power of 100 mW/cm^2 at ambient temperatures. The bleached signals were recorded using the given protocols and after another irradiation with the same dose, the unbleached signal after a 500 s pause was recorded. The bleached signals are normalized to the second measurement carried out with the same time delay between end of irradiation and start of measurement to correct the impact of signal fading. The decay curves are displayed in Fig. 9.

Using the usual integration interval the residual signals were calculated and the results of the optical stability tests are shown in Table 4.

4. Conclusions and outlook

The dosimetric properties, such as the intrinsic zero dose signals and the radiation induced signals of the Ta-IRSL and Ta-VSL protocol at different readout temperatures were systematically investigated. Zero doses, which range between 0.007 Gy (Ta-IRSL@100°C) and 0.136 Gy (Ta-VSL@200°C), are relatively low for both protocols and increase with increasing readout temperatures, which was also found in the Ta-BSL measurements in Kim et al. [32]. Further research is necessary using more glass samples in order to quantify the spread on the zero doses and estimating the detection limit. The deconvolution of the decay curves indicates a systematic decrease of the signal intensity and systematic increase

Table 3
Ratio of the remained Ta-OSL signal after one week of storage of the glass aliquots.

	Residual signal after 7.2 days of storage (signal fading factor)
Ta-IRSL@100°C	0.08
Ta-IRSL@200°C	0.48
Ta-IRSL@300°C	0.67
Ta-VSL@100°C	0.60
Ta-VSL@200°C	0.78
Ta-VSL@300°C	0.95

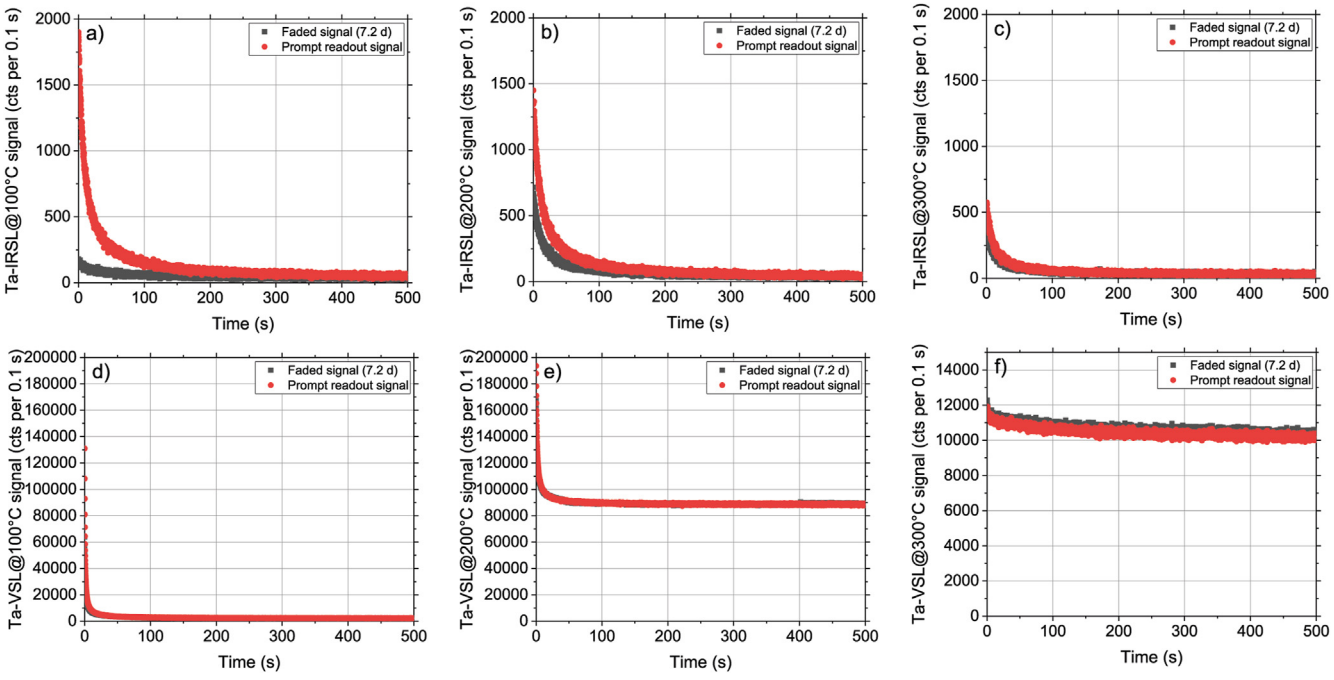

Fig. 8. a–f: Decay curves of the Ta-IRSL and Ta-VSL signals after 7.2 days storage and prompt readout.

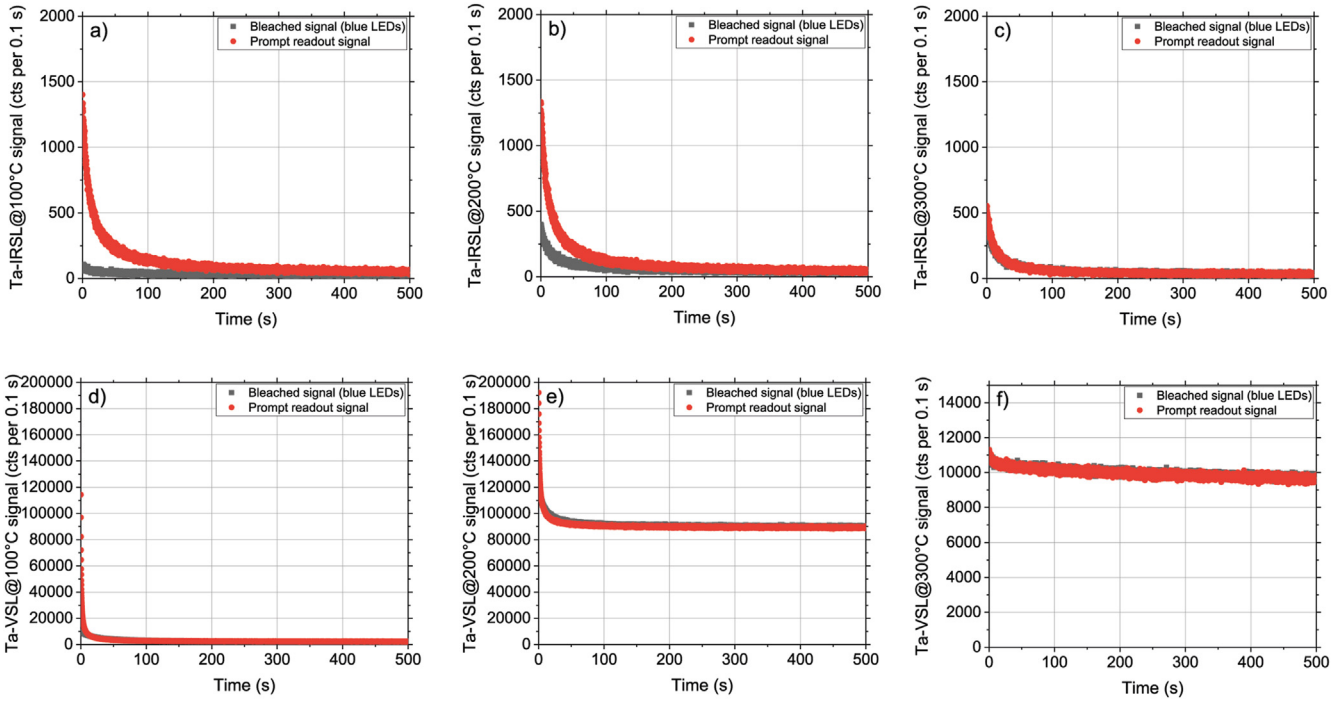

Fig. 9. a–f: Decay curves of the Ta-IRSL and Ta-VSL signals after 500 s bleaching of the blue LEDs (100 mW/cm^2 optical power) and readout without bleaching but 500 s pause.

Table 4
Ratio of the remained signals after 500 s bleaching of the blue LEDs of the reader with the maximum power of 100 mW/cm^2.

	Residual signal after blue bleaching
Ta-IRSL@100°C	0.05
Ta-IRSL@200°C	0.28
Ta-IRSL@300°C	0.85
Ta-VSL@100°C	0.15
Ta-VSL@200°C	0.56
Ta-VSL@300°C	0.75
500 s blue pre-bleaching TL	0.78

of an offset with increasing readout temperatures for the Ta-BSL and Ta-VSL protocols, which are not observed for the Ta-IRSL protocol. Reproducibilities are in the range between 0.97 and 1.03 (Ta-IRSL, all three readout temperatures) and 0.93 and 1.06 (Ta-VSL, 100 and 200 °C readout temperatures). All protocols indicate a linear dose response with a strong correlation, except for the Ta-VSL@300°C protocol. The signal stability test shows that the signal stability (samples stored in the dark at ambient temperatures) is correlated to the readout temperatures, and the remained signals after 7 days range between 0.08 (Ta-IRSL@100°C) and 0.95 (Ta-VSL@300°C). The optical stability test indicates that the signal bleaching is correlated to the readout temperatures, and the remained signals after blue LEDs bleaching with 100 mW/cm^2 optical power range between 0.05 (Ta-IRSL@100°C) and 0.75 (Ta-VSL@300°C). In general, the dosimetric properties, such as the reproducibility and linear dose response are fulfilled for most protocols, however, there are pro and cons of the presented Ta-OSL protocols, which have to be verified using realistic irradiation tests for dose recovery in the future investigations.

Declaration of competing interest

The authors declare that they have no known competing financial interests or personal relationships that could have appeared to influence the work reported in this paper.

Acknowledgements

The study was mainly carried out under the National Long- & Intermediate-Term Project of Nuclear Energy Development of Ministry of Science and ICT, Republic of Korea (No.2017M2A8A4015255) and the Nuclear Safety Research Program through the Korea Foundation Of Nuclear Safety (KoFONs) (No.1803014). The scientific cooperation is partially conducted in the framework of EPU (Eurasia-Pacific UNINET) network and partially funded by funds of the Federal Ministry of Education, Science and Research (BMBWF) Austria (project periods: 2020/2021).

References

[1] B.B. Williams, A.B. Flood, I. Salikhov, K. Kobayashi, R. Dong, K. Rychert, G. Du, W. Schreiber, H.M. Swartz, In vivo EPR tooth dosimetry for triage after a radiation event involving large populations Radiat, Environ. Biophys. 53 (2014) 335–346.
[2] F. Trompier, A. Romanyukha, R. Reyes, H. Vezin, F. Queinnec, D. Gourier, State of the art in nail dosimetry: free radicals identification and reaction mechanisms Radiat, Environ. Biophys. 53 (2014) 291–303.
[3] S.W.S. McKeever, S. Sholom, J.R. Chandler, Developments in the use of thermoluminescence and optically stimulated luminescence from mobile phones in emergency dosimetry Radiat, Prot. Dosim. 192 (2) (2020) 205–235.
[4] I.K. Bailiff, S. Sholom, S.W.S. McKeever, Retrospective and emergency dosimetry in response to radiological incidents and nuclear mass-casualty events: a review Radiat, Meas 94 (2016) 83–139.
[5] E.A. Ainsbury, E. Bakhanova, J.F. Barquinero, M. Brai, V. Chumak, V. Correcher, F. Darroudi, P. Fattibene, G. Gruel, I. Guclu, S. Horn, A. Jaworska, U. Kulka, C. Lindholm, D. Lloyd, A. Longo, M. Marrale, O. Monteiro Gil, U. Oestreicher, J. Pajic, B. Rakic, H. Romm, F. Trompier, I. Veronese, P. Voisin, A. Vral, C.A. Whitehouse, A. Wieser, C. Woda, A. Wojcik, K. Rothkamm, Review of retrospective dosimetry techniques for external ionising radiation exposures Radiat, Prot. Dosim. 147 (2011) 573–592.
[6] C. Bassinet, C. Woda, E. Bortolin, S. Della Monaca, P. Fattibene, M.C. Quattrini, B. Bulanek, D. Ekendahl, C.I. Burbidge, V. Cauwels, E. Kouroukla, T. Geber-Bergstrand, A. Mrozik, B. Marczewska, P. Bilski, S. Sholom, S.W.S. McKeever, R.W. Smith, I. Veronese, A. Galli, L. Panzeri, M. Martini, Retrospective radiation dosimetry using OSL of electronic components: results of an inter-laboratory

comparison Radiat, Meas 71 (2014) 475–479.
[7] D. Ekendahl, B. Bulánek, L. Judas, Comparative measurements of external radiation exposure using mobile phones, dental ceramic, household salt and conventional personal dosemeters Radiat, Meas 72 (2015) 60–65.
[8] A. Mrozik, B. Marczewska, P. Bilski, W. Gieszczyk, Investigation of OSL signal of resistors from mobile phones for accidental dosimetry Radiat, Meas 71 (2014a) 466–470.
[9] A.S. Pradhan, J.I. Lee, J.L. Kim, Use of OSL and TL of electronic components of portable devices for retrospective accident dosimetry Defect, Diffus. Forum 347 (2014) 229–245.
[10] S. Sholom, S.W.S. McKeever, Emergency OSL dosimetry with commonplace materials Radiat, Meas 61 (2014) 33–51.
[11] A. Pascu, S. Vasiliniuc, M. Zeciu-Dolha, A. Timar-Gabor, The potential of luminescence signals from electronic components for accident dosimetry Radiat, Meas 56 (2013) 384–388.
[12] D. Ekendahl, L. Judas, Retrospective dosimetry with alumina substrate from electronic components Radiat, Prot. Dosim. 150 (2) (2012) 134–141.
[13] C. Woda, I. Fiedler, T. Spöttl, On the use of OSL of chip card modules with molding for retrospective and accident dosimetry Radiat, Meas 47 (11–12) (2012) 1068–1073.
[14] F. Trompier, C. Bassinet, S. Della Monaca, A. Romanyukha, R. Reyes, I. Clairand, Overview of physical and biophysical techniques for accident dosimetry Radiat, Prot. Dosim. 144 (1–4) (2011) 571–574.
[15] F. Trompier, S. Della Monaca, P. Fattibene, I. Clairand, EPR dosimetry of glass substrate of mobile phone LCDs Radiat, Meas 46 (9) (2011) 827–831.
[16] I. Fiedler, C. Woda, Thermoluminescence of chip inductors from mobile phones for retrospective and accident dosimetry Radiat, Meas 46 (12) (2011) 1862–1865.
[17] C. Woda, C. Bassinet, F. Trompier, E. Bortolin, S. Della Monaca, P. Fattibene, Radiation-induced damage analysed by luminescence methods in retrospective dosimetry and emergency response Ann, Ist. Super. Sanità 45 (3) (2009) 297–306.
[18] H. Kim, M.C. Kim, J. Lee, I. Chang, S.K. Lee, J.L. Kim, Thermoluminescence of AMOLED substrate glasses in recent mobile phones for retrospective dosimetry Radiat, Meas 122 (2019) 53–56.
[19] C. Bassinet, N. Pirault, M. Baumann, I. Clairand, Radiation accident dosimetry: TL properties of mobile phone screen glass Radiat, Meas 71 (2014) 461–465.
[20] M. Discher, M. Greiter, C. Woda, Photon energy dependence and angular response of glass display used in mobile phones for accident dosimetry Radiat, Meas 71 (2014) 471–474.
[21] M. Discher, C. Woda, Thermoluminescence emission spectrometry of glass display in mobile phones and resulting evaluation of the dosimetric properties of a specific type of display glass Radiat, Meas 71 (2014) 480–484.
[22] A. Mrozik, B. Marczewska, P. Bilski, M. Klosowski, Investigation of thermoluminescence properties of mobile phone screen displays as dosimeters for accidental dosimetry Radiat, Phys. Chem. 104 (2014) 88–92.
[23] M. Discher, C. Woda, I. Fiedler, Improvement of dose determination using glass display of mobile phones for accident dosimetry Radiat, Meas 56 (2013) 240–243.
[24] M. Discher, C. Woda, Thermoluminescence of glass display from mobile phones for retrospective and accident dosimetry Radiat, Meas 53–54 (2013) 12–21.
[25] C. Bassinet, F. Trompier, I. Clairand, Radiation accident dosimetry on glass by TL and EPR spectrometry Health, Phys 98 (2) (2010) 400–405.
[26] J.R. Chandler, S. Sholom, S.W.S. McKeever, H.L. Hall, Thermoluminescence and phototransferred thermoluminescence dosimetry on mobile phone protective touchscreen glass, J. Appl. Phys. 126 (2019), 074901.
[27] S.W.S. McKeever, R. Minniti, S. Sholom, Phototransferred thermoluminescence (PTTL) dosimetry using Gorilla glass from mobile phones Radiat, Meas 106 (2017) 423–430.
[28] M. Discher, E. Bortolin, C. Woda, Investigations of touchscreen glasses from mobile phones for retrospective and accident dosimetry Radiat, Meas 89 (2016) 44–51.
[29] S. Sholom, S.W.S. McKeever, J.R. Chandler, OSL dosimetry with protective glasses of modern smartphones: a fiber-optic, non-destructive approach Radiat, Meas 136 (2020) 106382.
[30] C. Bassinet, W. Le Bris Tl, Investigation of glasses from mobile phone screen protectors for radiation accident dosimetryRadiat, Meas 136 (2020) 106384.
[31] M. Discher, M. Hiller, C. Woda, MCNP simulations of a glass display used in a mobile phone as an accident dosimeter Radiat, Meas 75 (2015) 21–28.
[32] H. Kim, M. Discher, M.C. Kim, C. Woda, J. Lee, Thermally assisted optically stimulated luminescence protocol of mobile phone substrate glasses for accident dosimetry, Radiat. Meas. 146 (2021), https://doi.org/10.1016/j.radmeas.2021.106625. In press.
[33] D. Richter, A. Richter, K. Dornich, Lexsyg – A new system for luminescence research Geochronometria 40 (4) (2013) 220–228.
[34] G.S. Polymeris, Thermally assisted OSL (TA-OSL) from various luminescence phosphors; an overview, Radiat. Meas. 90 (2016) 145–152.
[35] G.S. Polymeris, E. Şahiner, N. Meriç, G. Kitis, Experimental features of natural thermally assisted OSL (NTA-OSL) signal in various quartz samples; preliminary results, Nuclear Instruments and Methods in Physics Research Section B: Beam Interactions with Materials and Atoms 349 (2015) 24–30.